The Plant Cell, Vol. 9, 157–169, February 1997 © 1997 American Society of Plant Physiologists

Dynamics of Phragmoplastin in Living Cells during Cell Plate Formation and Uncoupling of Cell Elongation from the Plane of Cell Division

Xiangju Gu and Desh Pal S. Verma[1]

Department of Molecular Genetics, Ohio State Biochemistry Program and Plant Biotechnology Center, Ohio State University, Columbus, Ohio 43210

The cell plate is formed by the fusion of Golgi apparatus–derived vesicles in the center of the phragmoplast during cytokinesis in plant cells. A dynamin-like protein, phragmoplastin, has been isolated and shown to be associated with cell plate formation in soybean by using immunocytochemistry. In this article, we demonstrate that similar to dynamin, phragmoplastin polymerizes to form oligomers. We fused soybean phragmoplastin with the green fluorescence protein (GFP) and introduced it into tobacco BY-2 cells to monitor the dynamics of early events in cell plate formation. We demonstrate that the chimeric protein is functional and targeted to the cell plate during cytokinesis in transgenic cells. GFP–phragmoplastin was found to appear first in the center of the forming cell plate, and as the cell plate grew outward, it redistributed to the growing margins of the cell plate. The redistribution of phragmoplastin may require microtubule reorganization because the microtubule-stabilizing drug taxol inhibited phragmoplastin redistribution. Our data show that throughout the entire process of cytokinesis, phragmoplastin is concentrated in the area in which membrane fusion is active, suggesting that phragmoplastin participates in an early membrane fusion event during cell plate formation. Based on the dynamics of GFP–phragmoplastin, it appears that the process of cell plate formation is completed in two phases. The first phase is confined to the cylinder of the phragmoplast proper and is followed by a second phase that deposits phragmoplast vesicles in a concentric fashion, resulting in a ring of fluorescence, with the concentration of vesicles being higher at the periphery. In addition, overexpression of GFP–phragmoplastin appears to act as a dominant negative, slowing down the completion of cell plate formation, and often results in an oblique cell plate. The latter appears to uncouple cell elongation from the plane of cell division, forming twisted and elongated cells with longitudinal cell divisions.

INTRODUCTION

Cell plate formation during cytokinesis divides a cell anticlinally or periclinally and is a unique process in plants. During this process, Golgi apparatus–derived vesicles are transported to the equatorial region of the cell by phragmoplast microtubules (Hepler, 1982; Gunning and Wick, 1985; Kakimoto and Shibaoka, 1988). There, they first fuse with each other to form a continuous tubular network and then gradually consolidate into a flattened sheet in which callose is deposited (Samuels et al., 1995). As the membrane in the middle of the forming cell plate consolidates, phragmoplast microtubules reorganize and bring more new vesicles to the growing margin of the cell plate (Gunning and Wick, 1985). Therefore, membrane fusion during cell plate formation is a continuous process. At the early stage, when the cell plate is still confined inside the phragmoplast cylinder, the fusion events take place throughout the entire cell plate "disk." However, as the cell plate grows outward, membrane fusion events occur exclusively at the growing margin of the outwardly expanding cell plate.

Little is known about the molecular mechanism that brings about membrane fusion in plants, but the recent discovery that the syntaxin-related protein KNOLLE from Arabidopsis is involved in cytokinesis indicates a general machinery of vesicle fusion that might be conserved in plants (Lukowitz et al., 1996). Syntaxin is a plasma membrane protein that functions as a docking receptor (t-SNARE) for the synaptic vesicles during neurotransmitter release in mammalian cells. Syntaxin-like proteins play important roles in a number of membrane trafficking events ranging from neurotransmitter release to vacuole protein targeting (see Verma et al., 1994). A plant homolog of syntaxin has also been isolated by complementation of a yeast mutant (Bassham et al., 1995).

Although membrane fusion during cell plate formation has many properties similar to exocytosis (Baskin and Cande, 1990; Battey and Blackbourn, 1993; Verma and Gu, 1996), it

[1]To whom correspondence should be addressed at Plant Biotechnology Center, Rightmire Hall, Ohio State University, 1060 Carmack Road, Columbus, OH 43210-1002.

has several unique characteristics. Unlike the exocytosis event during secretion, membrane fusion at the cell plate results in the formation of a flattened membrane sac that creates an "extracellular" compartment inside the cell. The cargo (cell wall polysaccharides) that vesicles carry is deposited in this newly formed compartment. From electron microscopy studies, a new fusion structure called the dumbbell-shaped intermediate has recently been identified. This structure apparently arises by extending a tube from one vesicle to another and fusing the vesicles to form the tubulovesicular network (TVN) of the early cell plate (Samuels et al., 1995). This structure has never been observed during secretion or other exocytic events, indicating a unique process involved in the fusion of cell plate vesicles. Therefore, proteins that are not required for normal exocytic events may be required for cell plate formation.

One of these cell plate–specific proteins has been identified recently as phragmoplastin, which was localized to the cell plate in soybean root tip cells by using immunocytochemical methods (Gu and Verma, 1996). This protein shares significant homology with animal dynamin, a GTPase involved in endocytosis, as well as with VPS1, a protein required for Golgi-to-vacuole transport of vesicles in yeast (Rothman et al., 1990). It has been shown that animal dynamin participates in the pinching off of endocytic vesicles from the plasma membrane during receptor-mediated endocytosis (Herskovits et al., 1993; Van der Bliek et al., 1993). This process requires hydrolysis of GTP. In the presence of GTP-γ-S, however, the membrane fission event mediated by dynamin is blocked, resulting in the formation of elongated tubules on the plasma membrane. Electron microscopy localization studies have demonstrated that dynamin wraps around these elongated tubules (Takei et al., 1996). In addition, purified dynamin has been shown to be able to self-polymerize and form elongated helical structures in vitro (Hinshaw and Schmid, 1995).

The process of cell plate formation is one of the oldest biological processes that has been studied in living plant cells. By directly monitoring cell division in living cells, using phase contrast and interference microscopy, researchers have dissected the details of the process of cell plate formation at the morphological level. A variety of drugs that affect cell plate formation, for example, caffeine (Bonsignore and Hepler, 1985) and taxol (Yasuhara et al., 1993), has also been used to study this process. However, the involvement of various cellular components and the molecular mechanism of cell plate formation are not well understood. The exact event in which phragmoplastin participates during cell plate formation is not clear.

In this study, we used a fusion of phragmoplastin with the green fluorescence protein (GFP). The GFP–phragmoplastin fusion protein was found to be stable when expressed in transgenic tobacco cells. This allowed us to monitor the dynamics of GFP–phragmoplastin in the forming cell plate in living cells. These data, along with immunofluorescence localization, suggest that phragmoplastin participates in an early membrane fusion event during cell plate formation. This role is consistent with the temporal and spatial localization of phragmoplastin in the forming cell plate. These results also suggest a possible interaction of phragmoplastin with another protein(s). A number of mutants that affect the orientation of cell division are known (Smith et al., 1996), suggesting an involvement of many proteins that control vesicle fusion and cell plate orientation. We demonstrate that overexpression of phragmoplastin affects the plane of cell division and results in the formation of twisted cells with oblique cell plates or elongated cells with longitudinal cell divisions. Dissecting the roles of these proteins along with phragmoplastin may help us to understand the basic mechanism of cell plate orientation that may affect organogenesis and plant architecture.

RESULTS

Phragmoplastin Forms Oligomers in Vivo and Interacts with Another Protein(s)

Antibodies raised against soybean phragmoplastin (Gu and Verma, 1996) were used to react with cytosolic and membrane fractions from soybean and tobacco protein gel blots. In both tobacco BY-2 cells and soybean root extracts, a band with a molecular mass of ~68 kD was identified, indicating that this protein is conserved in plants (Figure 1A). A similar-sized protein with high homology to phragmoplastin has been identified, and it is encoded by an Arabidopsis cDNA (Dombrowski and Raikhel, 1995). When electrophoresed for a longer time, the band in the tobacco extract was separated into two bands, whereas that of soybean remained as one. Similar to that of soybean, phragmoplastin in tobacco cells was most abundant in the membrane fraction; a very low concentration of phragmoplastin was detected in the cytosolic fraction. Even though both of the two phragmoplastin bands in BY-2 cells were associated with the membrane fraction, the lower band could be partially (50%) extracted with Triton X-100 (Figure 1B, lane 2), whereas the upper band remained in the pellet (Figure 1B, lane 1). This suggests that phragmoplastin may exist in two forms in BY-2 cells.

Mammalian dynamin has been shown to polymerize in vitro and in vivo. Phragmoplastin oligomers can be detected by protein gel blotting after long storage of purified *Escherichia coli*–expressed phragmoplastin (Figure 1C, lane 3). To test whether phragmoplastin also polymerizes in vivo, cross-linking experiments were performed using 1-ethyl-3-(3-dimethylaminopropyl)carbodiimide (EDC). Several new bands that were not present in the control sample (Figure 1C, lane 1) were detected after EDC treatment followed by protein gel blot analysis (Figure 1C, lane 2). Together with the phragmoplastin monomer, these bands form an ascending ladder on the SDS gel that is comparable to that formed

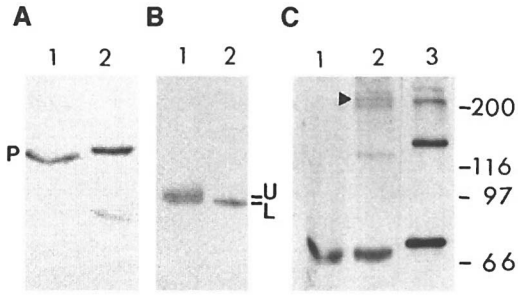

Figure 1. Protein Gel Blot Analysis of Phragmoplastin.

(A) Comparison of phragmoplastin from tobacco BY-2 cells and soybean roots. An antibody raised against soybean phragmoplastin recognizes similar molecular mass bands from both tobacco BY-2 cells (lane 1) and soybean roots (lane 2).

(B) Longer SDS-PAGE of tobacco phragmoplastin. Lane 1 contains a Triton X-100 (1%)–insoluble membrane fraction; lane 2, the Triton X-100–soluble fraction.

(C) Chemical cross-linking studies of phragmoplastin from tobacco cells. Lane 1 contains no EDC; lane 2, 100 mM EDC; lane 3, *E. coli*–expressed purified phragmoplastin (Gu and Verma, 1996) kept at −20°C without EDC.

The putative phragmoplastin dimer, trimer, and tetramers in lane 2 are comparable to those in lane 3, except for the difference in size due to the histidine linker in *E. coli*–expressed phragmoplastin. A phragmoplastin-associated protein (marked by arrowhead) is also cross-linked to the phragmoplastin complex in vivo. P, phragmoplastin monomer; U, upper band; L, lower band.

by the purified phragmoplastin in vitro, suggesting that these new protein bands are oligomers of phragmoplastin. An additional protein band (Figure 1C, lane 2, arrowhead) was found on the protein gel blot between the phragmoplastin trimer and tetramer, indicating that another protein(s) interacts with the phragmoplastin monomer or dimer in vivo.

Phragmoplastin Is Primarily Associated with Membranes throughout the Cell Cycle

To test whether there is any change in the association of phragmoplastin in BY-2 cells with the microsomal membrane fraction during different stages of the cell cycle, cells were synchronized at S phase, metaphase, and cytokinesis. As shown in Figures 2A to 2C, the frequency of cells in different stages, as revealed by 4′,6-diamidino-2-phenylindole (DAPI) staining, was >50%. The cells at these stages were fractionated into soluble and membrane fractions followed by protein gel blot analysis using phragmoplastin antibodies. No change in the membrane association of phragmoplastin was found; phragmoplastin was predominantly associated with the microsomal membrane fraction, with little or no activity in the soluble fraction throughout the cell cycle (Figures 2D to 2F). The ratio of the two bands did not change at any stage of the cell cycle (data not shown). The mechanism(s) involved in targeting phragmoplastin to the membrane fraction is not known because it has no putative transmembrane domains (Gu and Verma, 1996), but it could be due to the polymerization of phragmoplastin on the membranes, as demonstrated for mammalian dynamin (Tuma and Collins, 1995), or interaction with another membrane protein(s).

Temporal and Spatial Association of Phragmoplastin with Cell Plate Membrane Vesicles

By using immunofluorescence microscopy, we determined that the BY-2 cells exhibited a pattern identical to soybean (Gu and Verma, 1996) with respect to the localization of phragmoplastin. Cells in cytokinesis observed by staining with DAPI (Figure 3A) followed by a reaction with the microtubule antibody (Figure 3B) and phragmoplastin antibodies showed the presence of phragmoplastin between the two sets of the phragmoplast microtubules (Figure 3C). In the early stages of cell plate formation, phragmoplastin was present across the entire cell plate disc within the phragmoplast proper, but as the cell plate grew outward, phragmoplastin was concentrated

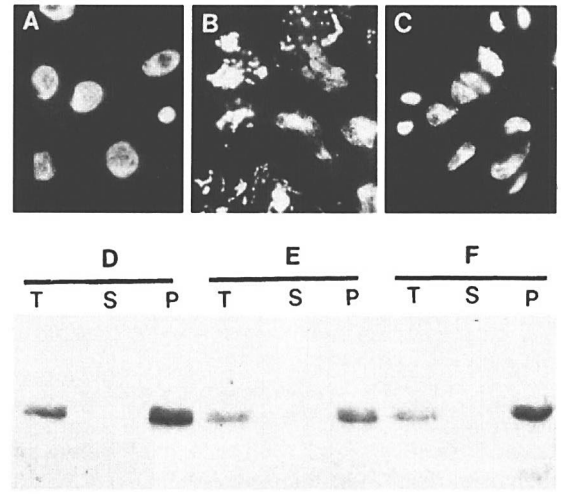

Figure 2. Association of Phragmoplastin with the Microsomal Fraction during the Cell Cycle.

(A) to **(C)** DAPI staining showing cells at different stages of the cell cycle. Cells after aphidicolin treatment (S phase) are shown in **(A)**. Cells after propyzomide treatment (just before metaphase) are shown in **(B)**. The small bright dots are the condensed chromosomes. Cells 90 mins after the release from propyzomide (at cytokinesis) are shown in **(C)**.

(D) to **(F)** Protein gel blot analysis showing the association of phragmoplastin with the membrane fraction at different stages of the cell cycle. T, total extract; S, S100; P, P100. **(D)** to **(F)** represent the same stages shown in **(A)** to **(C)**, respectively.

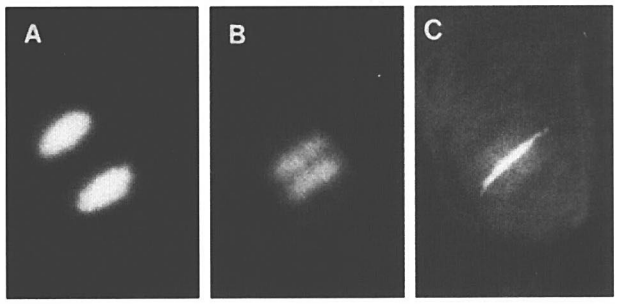

Figure 3. Immunofluorescence Localization of Phragmoplastin in Tobacco BY-2 Cells.

(A) Nuclear material (DAPI staining).
(B) Microtubules.
(C) Phragmoplastin.
The microtubule region is also slightly stained with phragmoplastin antibodies in **(C)**, whereas the nuclear region is not.

more on the growing margins of the cell plate, whereas the concentration in the middle of the cell plate decreased. A ringlike distribution pattern of phragmoplastin was observed at this stage in many cells (see below). This distribution correlated with the deposition and fusion of newly arrived vesicles on the forming cell plate. These results are identical to those observed with soybean root tips (Gu and Verma, 1996), suggesting conservation of this process in plants. Also, as cell plate formation was completed, phragmoplastin disappeared, and only a perinuclear diffused pattern of phragmoplastin was visible in the nondividing cells (data not shown). Because the concentration of phragmoplastin does not change significantly during the cell cycle, its recruitment into the vesicles that form the cell plate is a highly controlled spatial and temporal process.

The GFP–Phragmoplastin Fusion Protein Is Specifically Targeted to the Forming Cell Plate

To confirm the immunocytochemistry data and to study the dynamics of phragmoplastin distribution during cytokinesis in living cells, a GFP–phragmoplastin chimeric gene was constructed and transformed into tobacco BY-2 cells via Agrobacterium. Figure 4A shows the construct used in this experiment, and the expression of the GFP–phragmoplastin fusion protein in different transgenic cell lines is shown in Figure 4B. Upon longer exposure, all transgenic lines except that shown in lane 1 were found to express GFP–phragmoplastin. Approximately 50% of the kanamycin-resistant cell lines tested were found to express the GFP–phragmoplastin fusion protein at a significant level, and three lines (Figure 4B, lanes 2, 3, and 10) clearly overexpressed this chimeric protein. Cell lines 3 and 10 were used for further studies (Figures 5 to 7).

The GFP–phragmoplastin fusion protein seems very stable in BY-2 cells, even though a degradation product of native phragmoplastin was found in most of the preparations (Figure 4B, open arrowhead). No degradation products of GFP–phragmoplastin were detected by protein gel blot analysis. The degradation products of native phragmoplastin were not detected if the cell extract was made in the presence of proteinase inhibitors (see Figure 1). Similar to the native phragmoplastin, the GFP–phragmoplastin fusion protein was predominantly associated with the microsomal membrane fraction (data not shown).

Fluorescence microscopy studies showed that all cell lines expressing GFP–phragmoplastin fusion protein at a high level exhibited bright green fluorescence on the cell plate during cytokinesis (Figures 5A and 5B), whereas no green fluorescence was detected in the untransformed BY-2 cells. To ensure that the targeting of the GFP–phragmoplastin fusion protein to the cell plate was not due to the GFP part of the protein, we also transformed BY-2 cells with GFP alone and monitored the fluorescence in the transgenic cell lines expressing GFP. Although strong green fluorescence was observed in the cytoplasm of these cells, a clear dark line in the cell plate region was detected in the cells undergoing cytokinesis (Figure 5C, arrowheads), suggesting that the targeting of GFP–phragmoplastin to the cell plate is the function of

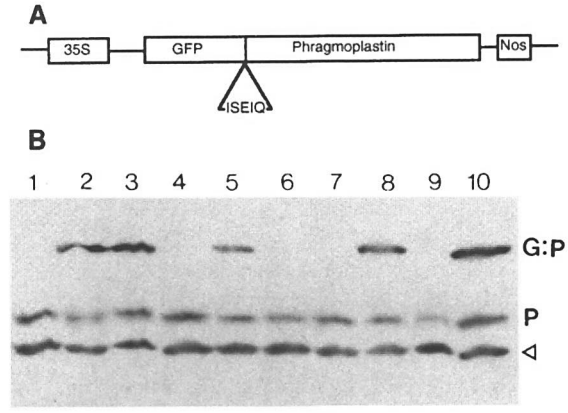

Figure 4. Expression of GFP–Phragmoplastin in Transgenic Tobacco BY-2 Cells.

(A) Diagram showing the GFP–phragmoplastin chimeric gene construct used to transform BY-2 cells. The amino acid sequence between GFP and phragmoplastin (ISEIQ, the linker region) is also shown. Nos, nopaline synthase; 35S, CaMV 35S promoter.
(B) Protein gel blot detection of the chimeric protein in different transgenic cell lines. The arrowhead shows the degradation product of the native protein. Upon longer exposure, the GFP–phragmoplastin band was detected in all lanes except lane 1, which did not express any GFP–phragmoplastin. G:P, GFP–phragmoplastin fusion protein; P, native phragmoplastin.

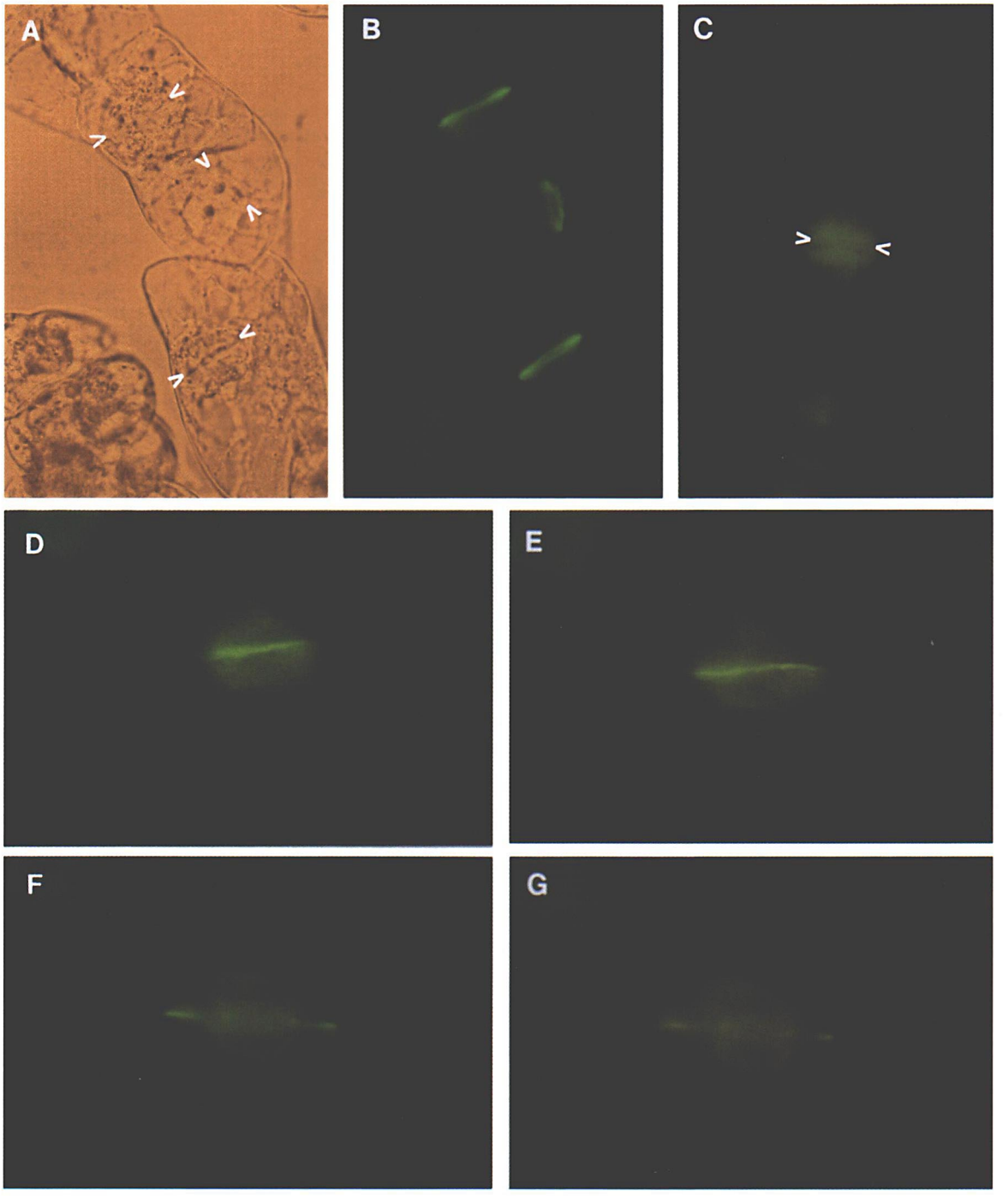

Figure 5. Localization of GFP–Phragmoplastin in Living Transgenic Tobacco Cells during Cytokinesis.

(A) and **(B)** GFP–phragmoplastin—expressing cells. **(A)** provides a bright-field image. Arrowheads indicate the position of the cell plates. **(B)** is a fluorescence image.

(C) Fluorescence image of a GFP-expressing cell undergoing cytokinesis. Arrowheads indicate the position of the cell plate, where no fluorescence was observed.

(D) to **(G)** Redistribution of phragmoplastin during cell plate growth. The same cell was recorded at different time intervals: 0 min **(D)**, 30 min **(E)**, 60 min **(F)**, and 90 min **(G)**.

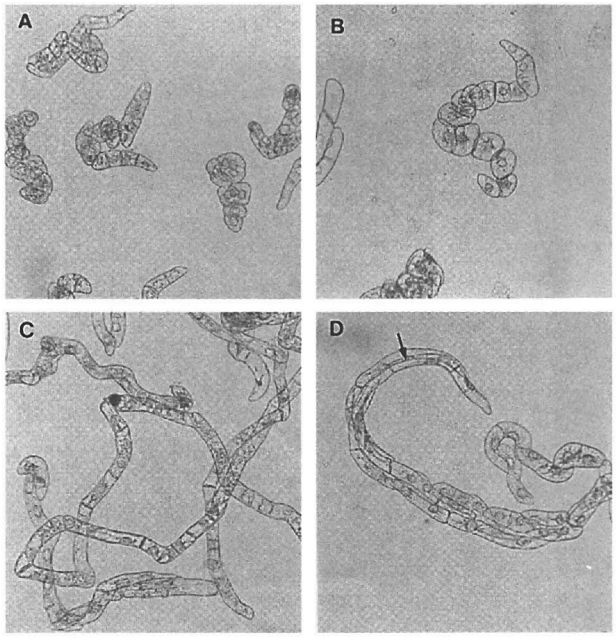

Figure 6. Morphologies of the GFP–Phragmoplastin—Expressing Cells in Liquid Culture during Log Phase.

(A) Tobacco BY-2 control cells.
(B) BY-2 cells expressing the GFP protein alone.
(C) and **(D)** GFP–phragmoplastin—overexpressing cells. The arrow indicates the longitudinal cell wall.

the phragmoplastin part of the fusion protein. This allowed us to monitor the dynamics of cell plate formation and the distribution of phragmoplastin during this process.

The GFP–phragmoplastin fusion protein appeared as a dense short line in the early stages of cell plate formation, marking the beginning of the process of vesicle fusion in the center of the phragmoplast. In later stages, however, the fluorescence was found concentrated at the two ends, suggesting that phragmoplastin was being targeted to the margins of the outwardly expanding cell plate. This was best demonstrated in some tilted cells, where a ringlike pattern was observed (Figure 5B; see also Figure 7B). These results agreed with the immunocytochemistry data and thus demonstrated that soybean phragmoplastin is able to participate functionally in cell plate formation in tobacco cells and presumably interacts with native phragmoplastin and other proteins. The concentration of phragmoplastin at the growing margin of the cell plate coincided temporally and spatially with the early membrane fusion events, which begin in the center and continue on at the periphery of the growing cell plate. During other stages of cell cycles, phragmoplastin appeared to be localized in the perinuclear region (data not shown) and is not concentrated in any area but rather is diffused, as observed by immunicytochemistry (Gu and Verma, 1996).

Phragmoplastin Is Redistributed from the Center to the Growing Margin of the Forming Cell Plate

The dynamics of GFP–phragmoplastin in transgenic, living BY-2 cells during cytokinesis were monitored using an inverted fluorescence microscope. The living cells were monitored in a culture chamber on a slide. The fluorescence of GFP–phragmoplastin on the cell plate remained stable for up to 2 hr in our experimental conditions. This allowed us to study the dynamics of phragmoplastin in vivo (Figures 5D to 5G). The green fluorescence first appeared in the center of the dividing cells soon after mitosis (Figure 5D) and gradually increased in intensity, forming a short line within 30 min (Figure 5E). As the cell plate expanded outward, the fluorescence in the center of the cell plate decreased, while the intensity of the fluorescence at the margin of the cell plate increased (Figures 5F and 5G). A clear redistribution of green fluorescence from the center to the periphery of the cell plate was observed. Because there was no change in the total phragmoplastin level during the cell cycle but there was a gradual decrease in the overall intensity of the GFP–phragmoplastin ring as the cell plate enlarged, it is very likely that the same molecules of phragmoplastin that participated in the early cell plate formation in the center of the phragmoplast were recycled to the periphery of the cell plate as the cell plate grew outward. This is consistent with our previous immunocytochemical studies in which the early cell plate stained much more strongly than did the late cell plates (see Gu and Verma, 1996). If this is the case, then phragmoplastin would be another protein besides tubulin to be recycled during cell plate formation.

GFP–phragmoplastin was found to be associated only with the forming cell plate. After the cell plate reached the parental cell wall, the green fluorescence gradually disappeared (data not shown). The dynamics of GFP–phragmoplastin in living cells thus suggests that throughout the entire process of cell plate formation, phragmoplastin is primarily concentrated at the area where vesicle fusion events take place—in the center on the early cell plate and at the periphery as the cell plate grows outward. The dynamics of GFP–phragmoplastin also showed that the cell plate is formed in two stages (Figures 5D to 5G). The first stage is confined to the center of the phragmoplast proper and is followed by the redistribution of phragmoplastin to the growing edge of the cell plate. Because microtubules are known to be involved in the expansion of the cell plate and serve as a carrier of vesicles, they may facilitate the redistribution of phragmoplastin (see below). The second phase extends the cell plate beyond the phragmoplast proper, and because the size of the cell plate may vary depending on the size of the cell, this phase may take different amounts of time for completion.

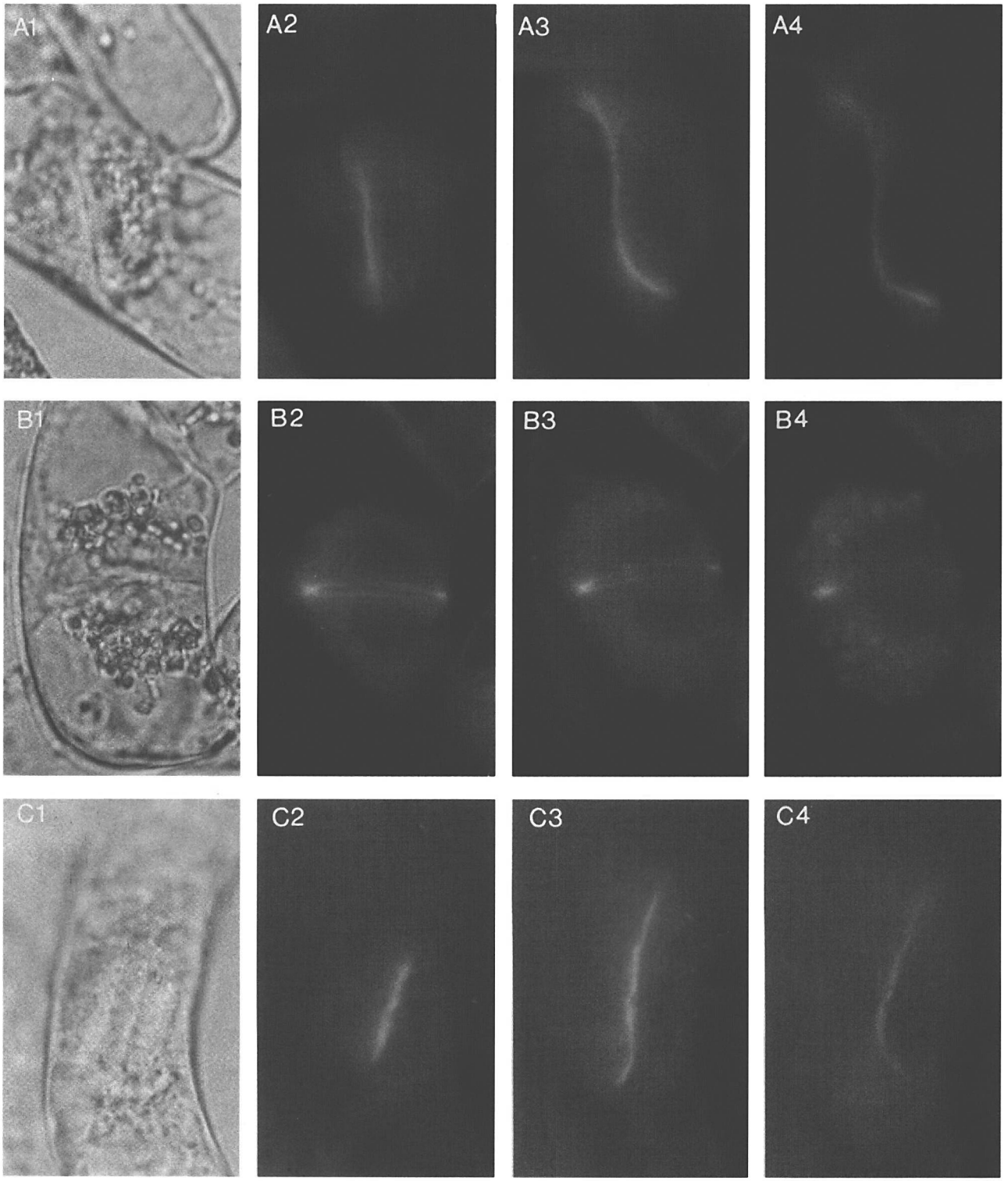

Figure 7. Effect of Caffeine and Taxol on the Redistribution of Phragmoplastin during Cell Plate Formation.

(A2) to **(A4)** Time course of control cells expressing GFP–phragmoplastin at 0, 60, and 120 min, respectively.
(B2) to **(B4)** Time course after taxol treatment at 0, 60, and 120 min, respectively.
(C2) to **(C4)** Time course after caffeine treatment at 0, 60, and 120 min, respectively.
(A1), **(B1)**, and **(C1)** are bright-field images of control, taxol-treated, and caffeine-treated GFP–phragmoplastin–expressing cells, respectively. The rest are fluorescence images. Note the oblique cell plate in **(A)** and the longitudinally oriented (periclinal) cell plate in **(C)**.

Overexpression of GFP–Phragmoplastin Slows Down Completion of the Cell Plate and Results in Oblique Cell Plate Formation

We observed that overexpression of GFP–phragmoplastin affects cell plate formation. In the two independent cell lines that had the highest level of expression of GFP–phragmoplastin (Figure 4, lanes 3 and 10), the completion of the cell plate was slowed down significantly. This was determined by observing living cells of lines 3 and 10 under the microscope as they completed cell plate formation. Normally, liquid culture of wild-type BY-2 cells contains small clusters of six to eight cells (Figure 6A). The morphology of the cells expressing GFP alone is not affected (Figure 6B). In contrast, chains of cells comprising >20 cells were frequently observed in GFP–phragmoplastin—expressing lines (Figures 6C and 6D). The cell wall boundary between daughter cells in these chains is not as clear as in the wild-type cells, apparently because of very thin cell walls. Often, oblique and even longitudinally oriented (periclinal) cell plates (cell walls) were seen in these cells (Figure 6D). The change in the orientation of the cell plate apparently had no effect on the direction of cell elongation. Cells continued to elongate in the original direction as if the cell plate were correctly oriented. Interestingly, in GFP–phragmoplastin—overexpressing cells, the cell plate sometimes changes its direction of growth during the late stage of cell plate formation, resulting in the formation of an S-shaped cell plate (Figure 7A). As a result, cells became elongated and twisted with each other to form nematode-like structures (Figures 6C and 6D).

These structures represent a transient stage, and cells eventually separated from each other and continued to divide. No phenotype was observed in GFP-overexpressing cells used as controls, except that these cells had higher fluorescence than did the GFP–phragmoplastin—expressing cells. Overexpression of GFP–phragmoplastin thus seems to have a dominant negative effect that was only observed in very actively dividing cells in which the expression of the fusion protein was at its highest levels and the time required for completing one cell cycle was at its lowest. The data also suggest that during its participation in the formation of the cell plate, phragmoplastin may interact with some other protein(s) that may play a role in determining the orientation of the cell plate. The fact that soybean phragmoplastin can functionally interfere with cell plate formation in tobacco cells suggests that phragmoplastin plays a central role in this fundamental process in plant cells.

Effects of Caffeine and Taxol on the Redistribution of Phragmoplastin

Caffeine and taxol are known to affect cell plate formation; however, their modes of action differ (Hepler and Bonsigore 1990; Yasuhara et al., 1993; Samuels and Staehelin, 1996). We tested the effects of these compounds on the redistribution of phragmoplastin in living cells by following the green fluorescence. Applying the microtubule-stabilizing drug taxol to the cell incubation chamber, once the cell plate was initiated immediately, "froze" the outward redistribution of phragmoplastin in these cells. The green ring of GPF–phragmoplastin remained stable in taxol-treated cells throughout the entire period of observation (up to 2 hr) without changing its shape or size, suggesting that the redistribution of phragmoplastin requires microtubule reorganization (Figure 7B) because taxol is known to affect microtubule depolymerization. In contrast, caffeine had no apparent effect on the early stage of the outward redistribution of phragmoplastin (Figure 7C). The fluorescence line of GFP–phragmoplastin elongated similarly to that in untreated cells. However, the redistribution of phragmoplastin from the center to the growing margin at the later stage was inhibited. No obvious increase in phragmoplastin at the growing margins of the caffeine-treated cells was observed as the cell plate grew outward. Before it reached the prenatal cell wall, the fluorescence on the cell plate started to disappear from the periphery inward. This is in sharp contrast with untreated cells, in which the fluorescence in the periphery increases while the fluorescence in the center decreases as cell division proceeds (Figure 7A; see also Figures 5D and 5G). Both caffeine and taxol were added to the cells once the cell plate had commenced (followed by GFP–phragmoplastin fluorescence). The effect of these drugs, however, may vary, depending on the time of treatment. The possible application of four-dimensional imaging methods with GFP–phragmoplastin—expressing cells by using wide-field computational optical sectioning microscopy followed by image deconvolution (Gens et al., 1996; McNally and Conchello, 1996; Thomas et al., 1996) may provide more insight into the dynamics of this process and the roles of various components.

DISCUSSION

Phragmoplastin Participates in an Early Event Associated with Vesicle Fusion during Cell Plate Formation

The latest model of cell plate formation in plants suggests five different steps: (1) the transport and arrival of Golgi apparatus–derived vesicles in the equatorial region, (2) the formation of thin dumbbell-shaped tubules leading to the TVN, (3) consolidation of the TVN into a smooth tubular network and fenestrated platelike structure filled with callose, (4) fusion of the margin of the cell plate with the parental cell membrane, and (5) synthesis of cellulose and the maturation of the cell plate into the cell wall (Samuels et al., 1995). Each of these steps has its own morphological characteristics, and the completion of each most likely requires different protein machinery and check points. For example, the transport of Golgi apparatus–derived vesicles requires phragmo-

plast microtubules as well as the microtubule-based motor proteins (Asada and Shibaoka, 1994). The consolidation of the TVN into a smooth tubular network likely requires the activation of a callose–cellulose synthase complex and the formation of callose (Samuels et al., 1995). Identifying a step in which a particular cell plate–associated protein participates is essential for understanding the function of that protein.

In this study, by using two different approaches (immunocytochemical localization in fixed cells and analyzing the distribution of GFP–phragmoplastin in living cells), we demonstrated that phragmoplastin is concentrated in the region of the cell plate in which active membrane fusion events take place. Phragmoplastin was detected immediately after the Golgi apparatus–derived vesicles begin to fuse to form the early cell plate disc which is confined to the phragmoplast cylinder. As the cell plate grows outward, phragmoplastin is redistributed to the growing margin of the cell plate. Both of these two regions (the early cell plates and the growing margin of the late cell plate) are where active vesicle fusion occurs and the TVN forms (Samuels et al., 1995).

Although both immunocytochemistry and GFP–phragmoplastin expression gave a similar pattern of localization during cell plate formation, the image of GFP–phragmoplastin was much clearer than that obtained by immunocytochemistry. We noticed in our previous immunocytochemistry studies (Gu and Verma, 1996) that the concentration of phragmoplastin in the growing margin is higher than that in the center in the late stages of cell plate growth. The dynamics of GFP–phragmoplastin in living cells showed unambiguously that phragmoplastin redistributes from the center and forms a ring at the edge of the expanding cell plate. The residual staining of phragmoplastin in the center of the late cell plates, as shown by immunocytochemistry, is most likely due to the lengthy fixation and incubation, which may cause proteins to diffuse.

Preliminary data obtained by using wide-field computational optical sectioning microscopy (conducted with S. Gens and B. Pickard, Washington University, St. Louis, MO) showed phragmoplastin to be associated with small, variable-sized and -shaped "bodies" clustered on both faces of the forming cell plate. This may represent a prefusion event of vesicles before fusion with the TVN or the extension of TVN.

Possible Role of Phragmoplastin in Cell Plate Formation

Dynamin in animals has been shown to form elongated tubules on the plasma membrane in the presence of GTP-γ-S (Takei et al., 1995). In the case of the Drosophila mutant *shibire*, specific amino acid substitutions in the primary sequence of dynamin prevent endocytosis and cause the formation of elongated tubules on the plasma membrane (Chen et al., 1991). This property of dynamin is due to its ability to polymerize and wrap around the biological membranes (Hinshaw and Schmid, 1995; Kelly, 1995; Takei et al., 1996). Interestingly, a fuzzy coat similar to that formed by animal dynamin on the plasma membrane tubules was also observed on the surface of the thin tubules of the TVN on the cell plate. However, the nature of this coat remains unclear (Samuels et al., 1995).

Phragmoplastin and dynamin share significant sequence homology, especially in the GTP binding domain and the so-called self-assembly motif (Nakayama et al., 1993; Gu and Verma, 1996). Our chemical cross-linking data indicated that similar to dynamin, phragmoplastin can also form oligomers on its own and appears to interact with another protein(s). Formation of the TVN involves dumbbell-shaped thin tubules connecting the vesicles. The tight temporal and spatial correlation between the formation of the TVN and the distribution of phragmoplastin suggests that phragmoplastin might be involved in the formation of these fusion tubules. We postulate that polymerization of phragmoplastin on the surface of the cell plate vesicles is likely to squeeze these vesicles into dumbbell-shaped tubular structures. Although these structures are difficult to preserve (Samuels et al., 1995), eventual immunolocalization of phragmoplastin on these tubules would be essential to confirm the role of this protein.

The level of phragmoplastin remains constant throughout the cell cycle, indicating that this protein might have other functions in the cell or that its activity is regulated by post-translational modifications. Our preliminary observation suggests that phragmoplastin may be phosphorylated, and this may play a role in its activity. The levels of other proteins involved in cell division, for example, cell cycle–related Cdc2, are also constant in dividing and stationary cells (Miao et al., 1993). Furthermore, it is not unusual for a protein to have seemingly different functions in the cell. Microtubules are one such example. Formation of the mitotic spindle and phragmoplasts and guiding cellulose fiber growth are only a few examples of the diverse functions that microtubules perform.

Possible Checkpoints in the Completion of the Cell Plate and Uncoupling of Cell Elongation from the Plane of Cell Division

The fact that caffeine treatment allows initial growth of the cell plate but affects its completion indicates that cell plate formation may involve specific checkpoints. From the data on the distribution of phragmoplastin at the forming cell plate, it appears that progression of the cell plate may be accomplished in two phases (Figure 8A). This is particularly evident in enlarged cells, where there is more space between the phragmoplast and the parental cell wall. In small cells, the nucleus has a larger volume, and the phragmoplast cylinder can fill the cell, almost touching the periphery, particularly during the transverse division. In such cells, the two phases are not very evident. In the first phase, the cell plate vesicles fuse with each other in the center of the phragmoplast to lay down the initial cell plate, stretching the width of the phragmoplast proper (Figure 8A, phase I). This

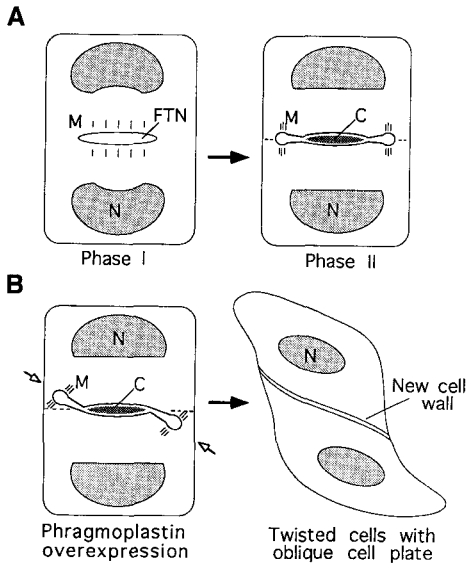

Figure 8. Diagram Showing the Main Stages of Cell Plate Formation in Which Phragmoplastin Plays a Role.

(A) Normal cell plate formation demonstrating two phases. Phase I represents the cell plate within the phragmoplast proper. Phase II represents growth of the cell plate. Overexpression of phragmoplastin affects phase II and results in oblique cell plate formation.

(B) Overexpression of phragmoplastin acting as dominant negative giving rise to twisted and elongated cells. The dashed lines indicate the position of the preprophase band with which the cell plate aligns. Open arrows indicate the orientation of the cell plate in GFP–phragmoplastin—overexpressing cells.

C, callose; FTN, fenestrated tubulonetwork; M, microtubules; N, nucleus.

is followed by outward growth accomplished by the redistribution of phragmoplastin and microtubules to the periphery of the growing cell plate (Figure 8A, phase II). This can be seen easily by GFP–phragmoplastin distribution in Figures 5D and 5G. A checkpoint between these two phases may control the redistribution of microtubules and phragmoplastin. It has been shown (Sack and Paolillo, 1985) that in Funaria, stomata are one celled because the separating wall is incomplete. In these cells, the cell plate forms normally in the center of the cell but never reaches the parent cell walls. A lack of cell plate initiation that occurs in nematode-feeding root cells, for example, results in multinucleate cells.

Overexpression of GFP–phragmoplastin acts as a dominant negative. In these cells, an oblique cell plate is formed that is longer than that in normal cells (Figure 8B). The ends of the cell plate begin to bend in opposite directions to form an S shape. Accordingly, the growing ends of the plate do not touch the cell wall rapidly, and the cell plate continues to grow. This results in an oblique or almost longitudinal cell division (see Figures 6D and 7A). The fact that these cells continue to elongate, irrespective of the orientation of cell division, demonstrates that the plane of cell division can be uncoupled from the direction of cell elongation. Understanding the molecular basis of this process may allow us to dissect the machinery that controls the orientation of cell division, which plays an important role in many plant developmental processes and organogenesis controlling the overall plant architecture.

GFP–Phragmoplastin as a New Tool to Study the Process of Cell Plate Formation

Phragmoplastin is a novel protein specifically localized on the cell plate. Fusion of this protein with GFP and the demonstration that this chimeric protein is stable in transgenic cells and targeted to the cell plate during cytokinesis provide a new tool to study the dynamics of cell plate formation. Because the fluorescence of the GFP is directly visible under a microscope without the lengthy fixation and incubation required for immunocytochemistry, it may reveal new insights, particularly into the coordination of steps involving phragmoplastin and the other cellular processes, such as the position of the preprophase band and the orientation of the cell plate.

Furthermore, the phase contrast and GFP–phragmoplastin images portray two different stages of cell plate formation. The GFP–phragmoplastin fluorescence image depicts the early events associated with vesicle fusion, whereas the phase contrast image portrays the consolidated cell plate disc as the cell plate matures. The latter is also visible by staining with aniline blue, a marker for callose deposition. These two images complement each other to give us a more detailed picture of the process of cell plate formation and may help us dissect various steps involved in making this structure.

The GFP–phragmoplastin—expressing transgenic cell lines will also be an excellent system in which to test a variety of drugs and herbicides affecting the process of cell plate formation or the kinetics of cell plate growth. Our data showed that taxol and caffeine, two well-known cell plate inhibitors, have dramatic and different effects on the redistribution of phragmoplastin on the cell plate. The effect of taxol is due to the stabilization of phragmoplast microtubules, but the mechanism of caffeine is not fully understood, although several explanations for the caffeine effect have been proposed (Hepler, 1982; Samuels et al., 1995). In our experiments, caffeine was clearly shown to inhibit the redistribution of phragmoplastin. It is possible that inhibition of the redistribution of phragmoplastin is the reason that caffeine blocks cell plate growth.

Transfer of GFP–phragmoplastin to Arabidopsis and the use of these transgenic lines may also be tools to study mutants that affect cell plate formation. By crossing Arabidopsis cytokinesis mutants such as *knolle* (Lukowitz et al., 1996) with GFP–phragmoplastin—expressing Arabidopsis lines and studying the distribution of GFP–phragmoplastin, one may be able to define the interaction of phragmoplastin and

other genes affecting cell plate formation during cytokinesis. GFP–phragmoplastin may also be useful for fractionating Golgi apparatus–derived vesicles targeted to the cell plate, which may help to dissect early biochemical and molecular events involved in the fusion of these vesicles and the initiation of synthesis and deposition of primary cell wall components. In any event, phragmoplastin is a new tool for dissecting the process of cell plate formation and determining the molecular mechanism involved in the completion of this last step in plant cell division.

METHODS

Synchronization of Tobacco BY-2 Cells

BY-2 cells were synchronized by the methods of Shibaoka (Asada and Shibaoka, 1994). Briefly, 5 mL of 2-day-old BY-2 cell culture was mixed with 20 μL of aphidicolin (2.5 mg/mL) and transferred to 15 mL of fresh Murashige and Skoog medium (Bethesda Research Laboratories, Gaithersburg, MD). Cells were allowed to grow for 24 hr, and then the drug was removed by filtration of cells on one layer of Miracloth (Calbiochem, San Diego, CA) and washed with 50 mL of fresh medium. Cells were then transferred to 20 mL of new medium. After 5 hr, 4 μL of propyzomide (6 mg/mL) was added to the medium. Cells were treated with propyzomide for 5 hr and then washed again as before and transferred into new medium. Cells in the cytokinesis stage were harvested after 90 min in the fresh medium. Cells after aphidicolin and propyzomide treatment were also harvested and extracted for phragmoplastin analysis by protein gel blotting.

Protein Gel Blot Analysis

BY-2 cells were ground in liquid nitrogen with a mortar and pestle and then homogenized in ice-cold TB buffer (25 mM Tris-HCl, pH 8.0, 5 mM EDTA, 1 mM β-mercaptoethanol, 0.5 mM phenylmethylsulfonyl fluoride, 1 mM leupeptin) containing 17% (w/v) sucrose. The homogenate was passed through one layer of Miracloth and centrifuged at 10,000*g* for 10 min. The pellet containing the nuclei, mitochondria, and cell debris was discarded, and the supernatant (S10) was centrifuged at 100,000*g* for 30 min to give a soluble fraction (S100) and microsomal pellet (P100). The microsomal pellet was then resuspended in the extraction buffer. Both the soluble fraction and the microsomal fractions (50 μg of protein each) were mixed with SDS sample buffer and subjected to SDS-PAGE. The microsomal pellet was also extracted with 1% Triton X-100 in TB buffer. The Triton X-100–soluble and the Triton X-100–insoluble fractions were separated by centrifugation and subjected to SDS-PAGE.

After electrophoresis, proteins were transferred to a Hybond-C membrane (Amersham, Arlington Heights, IL), and the phragmoplastin was detected using affinity-purified anti–soybean phragmoplastin antibody and the enhanced chemiluminescence protein gel blot system (Amersham).

Immunofluorescence Localization of Phragmoplastin

Three-day-old BY-2 cells were fixed in 4% paraformaldehyde in PHEM (60 mM Pipes, 25 mM Hepes, 10 mM EGTA, and 2 mM $MgCl_2$, pH 7.0) for 1 hr at room temperature and then washed with buffer (10 mM Mes, pH 5.7, 30 mM $CaCl_2$, 0.1% BSA, 5 mM β-mercaptoethanol, and 0.4 M mannitol) on one layer of Miracloth. Cells were then digested in a solution containing 1% cellulase (Calbiochem) and 0.1% pectolyase Y23 in washing buffer for 15 min. After rinsing with PHEM buffer, cells were transferred to poly-L-lysine–coated slides and air dried for 10 min. Immunofluorescence microscopy was then performed following standard methods using affinity-purified anti–soybean phragmoplastin IgG as the first antibody and fluorescein isothiocyanate (FITC)–conjugated anti–rabbit goat IgG as a second antibody as described by Gu and Verma (1996). Preimmune serum was used as the first antibody in the control group. For double-labeling experiments, mouse anti-tubulin IgG (Amersham) and tetramethylrhodamine isothiocyanate (TRITC)–conjugated goat anti–mouse IgG (Sigma) were used to stain microtubules. DNA was stained with 4′-6-diamidino-2-phenylindole (DAPI) at a concentration of 10 μg/mL for 5 min at room temperature. Photographs were taken using appropriate filters for FITC, TRITC, and DAPI fitted to a microscope (Carl Zeiss, Cincinnati, OH).

Chemical Cross-Linking

The microsomal fraction of tobacco BY-2 cells was treated with different concentrations of 1-ethyl-3-(3-dimethylaminopropyl)carbodiimide (EDC; 0, 1, 10, and 100 mM) on ice for 30 min. β-Mercaptoethanol was then added to the samples to stop the reaction (Tuma and Collins, 1995). The samples were mixed with SDS buffer and subjected to SDS-PAGE. Proteins were detected by protein gel blot analysis.

Green Fluorescence Protein–Phragmoplastin Fusion and Transformation of BY-2 Cells

The green fluorescence protein (GFP) coding region amplified from pBI-35S-mGFP (a gift from J. Haseloff, MRC Laboratory, Cambridge, UK) and cloned into plasmid pUC-GFP44 was cut out and cloned into the XbaI-SacI sites of pBI221-JR (both plasmids were kindly provided by Z. Yang, Ohio State University, Columbus). The resulting plasmid, pE-GFP44, contained a cauliflower mosaic virus 35S promoter, a GFP coding sequence with a BglII site at the C-terminal end, and a nopaline synthase terminator. The BglII-SacI fragment of phragmoplastin coding sequence was removed from plasmid pEPDL12 (Gu and Verma, 1996) and cloned into BglII-SacI sites of pE-GFP44 to give the plasmid pE-GFP44-PDL-BS. The XbaI-SacI fragment of the new plasmid was finally cloned into XbaI-SacI sites of plasmid pBI121-MLB-PDL12 (X. Gu and D.P.S. Verma, unpublished data) to give plasmid pBI121-EGP. The final plasmid contained a 35S promoter, a coding sequence for a GFP–phragmoplastin fusion protein, and a nopaline synthase terminator. The plasmid was transformed into *Agrobacterium tumefaciens* LBA4404 by using the frozen–thaw method.

Transformation of BY-2 cells was performed using the procedure of An et al. (1992). Five milliliters of 3-day-old BY-2 cells was mixed with 100 μL of Agrobacterium strain LBA4404 harboring the plasmid pBI121-EGP. The cells were allowed to grow in Petri plates at 25°C without shaking for 2 days. Cells were then washed with fresh medium on one layer of Miracloth to remove most of the bacteria and then plated on solid Murashige and Skoog medium containing 300 μg of kanamycin and 500 μg of carbenicillin. Transgenic calli usually emerged after 2 to 3 weeks. The calli were then transferred to new antibiotic-containing plates.

Detection of the GFP–Phragmoplastin in Transgenic Cell Lines

Transgenic cells (20 mg fresh weight) from different calli were digested in 200 μL of enzyme solution (1% cellulase, 10 mM Mes, pH 5.7, and 0.38 M sorbitol) for 20 min at room temperature. Cells were then centrifuged for 2 min in a microcentrifuge at room temperature. The enzyme solution was removed, and the cells were washed with 200 mL of washing solution (1% Triton X-100 in PHEM). After pelleting, the cells were directly solubilized in SDS sample buffer and processed for SDS-PAGE and protein gel blotting.

Detection of GFP–Phragmoplastin Fluorescence in Living Transgenic BY-2 Cells

The fluorescence of GFP–phragmoplastin was studied in cells grown on solid medium or in liquid medium, using an epifluorescence microscope equipped with an FITC filter set. From our experience, the fluorescence in the liquid-cultured cells was much stronger than that of the cells grown on the solid medium; therefore, most of our studies are based on the liquid-cultured cells. To follow the dynamics of the GFP–phragmoplastin in living cells, 100 μL of liquid-cultured cells was mixed with 100 μL of medium in a culture well on the slides. The cells were then monitored under an inverted microscope for 2 hr. To reduce photobleaching, an excitation light was turned on only when photographs were taken. For studying the effect of various drugs on cell plate formation, a dividing cell was first spotted and the fluorescence was recorded. Then 50 μL of caffeine (final concentration of 10 mM) or 10 μL of taxol (final concentration of 50 μM) was added. The same cell was then photographed at different time intervals.

ACKNOWLEDGMENTS

We thank Zhenbiao Yang for providing us with the plasmid constructs containing GFP developed in James Haseloff's laboratory and for helping with fluorescence microscopy. Technical assistance for BY-2 transformation by Reng Ju is appreciated. We thank Zonglie Hong for his generous help and comments on the manuscript. Critical comments by Zhenbiao Yang are much appreciated. This work was initiated with the support of National Science Foundation Grant No. DCB 8904101.

Received September 25, 1996; accepted December 20, 1996.

REFERENCES

An, G., Ebert, P.R., Mitra, A., and Ha, S.B. (1992). Binary vectors. In Plant Molecular Biology Manual, S.B. Gelvin, R.A. Schilperoort, and D.P.S. Verma, eds (Dordrecht, The Netherlands: Kluwer Academic Publishers), pp. A3/1–A3/19.

Asada, T., and Shibaoka, H. (1994). Isolation of polypeptides with microtubule-translocating activity from phragmoplasts of tobacco BY-2 cells. J. Cell Sci. **107,** 2249–2257.

Baskin, T.I., and Cande, W.Z. (1990). The structure and function of the mitotic spindle in flowering plants. Annu. Rev. Plant Physiol. Plant Mol. Biol. **41,** 277–315.

Bassham, D.C., Gal, S., Conceicao, A., and Raikhel, N.V. (1995). An Arabidopsis syntaxin homologue isolated by functional complementation of a yeast *pep*12 mutant. Proc. Natl. Acad. Sci. USA **92,** 7262–7266.

Battey, N.H., and Blackbourn, H.D. (1993). The control of exocytosis in plant cells. New Phytol. **123,** 307–338.

Bonsignore, C.L., and Hepler, P.K. (1985). Caffeine inhibition of cytokinesis: Dynamics of cell plate formation–deformation in vivo. Protoplasma **129,** 28–35.

Chen, M.S., Obar, R.A., Schroeder, C.C., Austin, T.W., Poodry, C.A., Wadsworth, S.C., and Vallee, R.A. (1991). Multiple forms of dynamin are encoded by *shibire*, a Drosophila gene involved in endocytosis. Nature **35,** 583–586.

Dombrowski, J.E., and Raikhel, N.V. (1995). Isolation of cDNA encoding a novel GTP-binding protein of *Arabidopsis thaliana.* Plant Mol. Biol. **28,** 1121–1126.

Gu, X., and Verma, D.P.S. (1996). Phragmoplastin, a dynamin-like protein associated with cell plate formation in plants. EMBO J. **15,** 695–704.

Gunning, B.E.S., and Wick, S.M. (1985). Preprophase bands, phragmoplast, and spatial control of cytokinesis. J. Cell Sci. **2** (suppl.), 157–179.

Hepler, P.K. (1982). Endoplasmic reticulum in the formation of the cell plate and plasmodesmata. Protoplasma **111,** 121–133.

Hepler, P.K., and Bonsigore, C.L. (1990). Caffeine inhibition of cytokinesis: Ultrastructure of cell plate formation/degradation. Protoplasma **157,** 182–192.

Herskovits, J.S., Burgess, C.C., Obar, R.A., and Vallee, R.B. (1993). Effects of mutant rat dynamin on endocytosis. J. Cell Biol. **122,** 565–578.

Hinshaw, J.E., and Schmid, S.L. (1995). Dynamin self-assembles into rings suggesting a mechanism for coated vesicle budding. Nature **374,** 190–192.

Kakimoto, T., and Shibaoka, H. (1988). Cytoskeletal ultrastructure of phragmoplast–nuclei complexes isolated from cultured tobacco cells. Protoplasma **2** (suppl.), 95–103.

Kelly, R.B. (1995). Ringing necks with dynamin. Nature **374,** 116–117.

Lukowitz, W., Mayer, U., and Jurgens, G. (1996). Cytokinesis in the Arabidopsis embryo involves the syntaxin related KNOLLE gene product. Cell **84,** 61–71.

McNally, J.G., and Conchello, J.-A. (1996). Confocal, two-photon and wide-field microscopy: How do they compare? Plant Physiol. **111,** 17.

Miao, G.-H., Hong, Z., and Verma, D.P.S. (1993). Two functional soybean genes encoding $p34^{cdc2}$ protein kinases are regulated by different developmental pathways. Proc. Natl. Acad. Sci. USA **90,** 943–947.

Nakayama, M., Yazaki, K., Kusano, A., Nagata, K., Hanai, N., and Ishihama, A. (1993). Structure of mouse Mx1 protein. J. Biol. Chem. **268,** 15033–15038.

Rothman, J.H., Raymond, T., O'Hara, P.J., and Stevens, T. (1990). Putative GTP-binding protein homologous to interferon-inducible Mx proteins performs an essential function in yeast protein sorting. Cell **61,** 1063–1074.

Sack, F.D., and Paolillo, D.J. (1985). Incomplete cytokinesis in the stomata of *Funaria*. Am. J. Bot. **72,** 1325–1333.

Samuels, A.L., and Staehelin, L.A. (1996). Caffeine inhibits cell plate formation by disrupting membrane reorganization just after the vesicle fusion step. Protoplasma **195,** 144–155.

Samuels, A.L., Giddings, T.H., and Staehelin, L.A. (1995). Cytokinesis in tobacco BY-2 and root tip cells: A new model of cell plate formation in higher plants. J. Cell Biol. **130,** 1345–1357.

Smith, L.G., Hake, S., and Sylvester, A.W. (1996). The *tangled-1* mutation alters cell division orientation throughout maize leaf development without altering leaf shape. Development **122,** 481–489.

Takei, K., McPherson, P.S., Schmid, S., and Camilli, P.D. (1995). Tubular membrane invaginations coated by dynamin rings are induced by GTP-γ-S in nerve terminals. Nature **374,** 186–190.

Takei, K., Mundigl, O., Daniell, L., and Camilli, P.D. (1996). The synaptic vesicle cycle: A single vesicle budding step involving clathrin and dynamin. J. Cell Biol. **133,** 1237–1250.

Thomas, C., DeVries, P., Hardin, J., and White, J. (1996). Four-dimensional imaging: Computer visualization of 3D movements in living specimens. Science **273,** 603–607.

Tuma, P.L., and Collins, C.A. (1995). Dynamin forms polymeric complexes in the presence of lipid vesicles. J. Biol. Chem. **270,** 26707–26714.

Van der Bliek, A.M., Redelmerier, T.E., Damke, H., Tisdale, E.J., Meyerowitz, E.M., and Schmid, S.L. (1993). Mutations in human dynamin block an intermediate stage in coated vesicle formation. J. Cell Biol. **122,** 553–563.

Verma, D.P.S., and Gu, X. (1996). Vesicle dynamics during cell plate formation in plants. Trends Plant Sci. **1,** 145–149.

Verma, D.P.S., Cheon, C.-I., and Hong, Z. (1994). Small GTP-binding proteins and membrane biogenesis in plants. Plant Physiol. **106,** 1–6.

Yasuhara, H., Sonobe, S., and Shiboaka, H. (1993). Effect of taxol on the development of cell plate and of the phragmoplast in tobacco BY-2 cells. Plant Cell Physiol. **34,** 21–29.